Geological Quarterly, 2025, 69, 58
DOI: https://doi.org/10.7306/gq.1831

Uncovering the sources of soil lead in the Old Copper Basin (SW Poland): insights from Pb isotope geochemistry

Katarzyna DERKOWSKA[1, 2, *], Anna PIETRANIK[2], Jakub KIERCZAK[2], Vojtěch ETTLER[3] and Martin MIHALJEVIČ[3]

[1] Polish Geological Institute – National Research Institute, Rakowiecka 4, 00-975 Warszawa, Poland; ORCID: 0000-0002-9459-4174

[2] University of Wrocław, Institute of Geological Sciences, Maxa Borna 9, 50-204, Wrocław, Poland; ORCID: 0000-0003-3990-8721 [A.P], 0000-0002-3243-6832 [J.K.]

[3] Charles University, Faculty of Science, Institute of Geochemistry, Mineralogy and Mineral Resources, Albertov 6, 128 00 Prague 2, Czechia; ORCID: 0000-0002-0151-0024 [V.E.], 0000-0002-4875-9345 [M.M.]

Derkowska, K., Pietranik, A., Kierczak, J., Ettler, V., Mihaljevič, M., 2025.Uncovering the sources of soil lead in the Old Copper Basin (SW Poland): insights from Pb isotope geochemistry. Geological Quarterly, 69, 58; https://doi.org/10.7306/gq.1831

Associate Editor: Justyna Ciesielczuk

This study explores lead (Pb) isotopic signatures in soils in the Old Copper Basin in SW Poland, an area influenced by centuries of copper mining and smelting. Previous observations showed that Pb distribution in these soils differs from distributions of other metallurgical contaminants such as Cu or Ni, suggesting additional sources of Pb. To address this, we conducted isotopic analyses of topsoil and subsoil samples, including EDTA-extractable fractions, as well as representative rocks and slags. Isotopic ratios ($^{206}Pb/^{207}Pb$ and $^{208}Pb/^{206}Pb$) were used to distinguish lithogenic, metallurgical, and atmospheric inputs. Subsoils displayed a wide isotopic range ($^{206}Pb/^{207}Pb$ = 1.183–1.234), commonly increasing with depth and consistent with local rocks and ore sources. Topsoils showed more uniform and less radiogenic values ($^{206}Pb/^{207}Pb$ = 1.172–1.193), forming a regionally consistent isotopic pattern that we define as the Lower Silesian Contemporary Pollution Signal (LSCPS). This signal is linked to long-range atmospheric deposition from industrial emissions. EDTA-leachable Pb in surface soils was isotopically less radiogenic than bulk $^{206}Pb/^{207}Pb$ and similar to LSCPS Pb, indicating mobility of this anthropogenic fraction. Some topsoil profiles outside direct mining areas showed elevated Pb with isotopic ratios not related to local ores or slags, pointing to external atmospheric sources. These results emphasize the complex origin of Pb contamination in post-industrial landscapes and demonstrate the value of Pb isotope geochemistry in tracing overlapping pollution signals.

Key-words: Pb isotopes, Cu ores, soil contamination, Zechstein Limestone Ca1, Kupferschiefer.

INTRODUCTION

Lead (Pb) isotopes are widely recognized as a robust tool for tracing the sources and pathways of Pb contamination in environmental systems. Their strength lies in the fact that both natural and anthropogenic Pb sources – such as ore deposits, volcanic emissions, smelting emissions, paints, and leaded gasoline – possess distinct isotopic compositions (e.g., Monna et al., 1999; Ettler et al., 2004; Komárek et al., 2008; Mihaljevič et al., 2009; Alyazichi et al., 2016). These differences, preserved in the relative abundances of radiogenic isotopes (^{206}Pb, ^{207}Pb, ^{208}Pb), serve as geochemical fingerprints that can distinguish between geogenic and anthropogenic inputs (Walraven et al., 2014; Cheyne et al., 2018). This isotopic approach has been successfully applied in many environmental studies to resolve complex contamination patterns and to quantify the contribution of specific pollution sources (Komárek et al., 2008; Mihaljevič et al., 2011; Tyszka et al., 2012, 2016; Kierczak et al., 2013, Abbaszade et al., 2022; Peng et al., 2022a, b).

In southwestern Poland, the historical Old Copper Basin (OCB), located within the North Sudetic Basin, is a region marked by centuries of polymetallic ore mining and processing. Previous studies (Potysz et al., 2018; Derkowska et al., 2023) have demonstrated a strong impact of historical metallurgical activity on surface metal loads. In our earlier environmental survey (Derkowska et al., 2023), the spatial distribution of Pb diverged from that of other smelting-related metals such as Cu and Ni, indicating that different sources or dispersal mechanisms may be responsible for Pb contamination. This observation highlights the need for isotopic tools to better resolve these differences.

* Corresponding author, e-mail: katarzyna.derkowska@pgi.gov.pl

Received: October 1, 2025; accepted: December 11, 2025; first published online: December 31, 2025

In this study, we apply Pb isotope geochemistry to a broad set of soils, rocks, and metallurgical residues collected from both contaminated and background sites across the OCB. Our main objective is to identify and distinguish between Pb sources: whether derived from local lithology, historical smelting waste, or regional atmospheric fallout. We hypothesize that the isotopic composition of these soils reflects contributions from at least two dominant Pb sources: deeper horizons retain lithogenic or ore-related signatures, while topsoils record a well-mixed, potentially isotopically distinct signal from long-range atmospheric deposition. Additionally, we propose that the contrast between bulk and EDTA-leached fractions will not only discriminate between immobile and mobile Pb pools, but also help track legacy contaminants that remain environmentally relevant. Finally, we explore the hypothesis that historical slags may locally imprint distinct isotopic signals in the subsoil, especially where weathering enhances Pb migration. This multi-proxy approach allows us to trace both the origin and environmental behavior of Pb in mining-impacted landscapes. To test this, we have analysed both bulk and EDTA-leached soil fractions in a set of vertical profiles and surface samples. We also include isotopic data from local rocks and slag materials to constrain potential endmembers. Although previous studies near the Legnica-Głogów Copper District have reported relatively homogeneous Pb isotope signatures in processed Kupferschiefer ores (Chrastný et al., 2010; Tyszka et al., 2012), the broader regional patterns – especially in forested and rural areas – remain underexplored.

Our study aims to address this gap by examining Pb isotopic composition in both contaminated and background soils, including soil profiles influenced by historical ore processing and those situated outside of the anthropogenic impact of former mining and smelting operations. By integrating isotopic ratios with chemical extractions and mineralogical observations, we explore the relative importance of industrial and lithogenic Pb sources, while also assessing the extent to which regional atmospheric inputs shape surface-soil isotopic signatures. This wider regional context allows us to interpret isotopic signals not only in terms of local smelter influence, but also in the framework of regional-scale contamination.

SITE DESCRIPTION

GEOLOGICAL SETTING

The research area is located in SW Poland, north of the Sudeten Mountains in the Kaczawa Foothills area, in a geological unit known as the North Sudetic Basin (NSB). The NSB is sorrounded from NE and S by Kaczawa Metamorphic Complex, which is located on the Fore-Sudetic Block, characterized by pre-Variscan age, metasedimentary and metavolcanic lithologies (Kryza et al., 2004). The NSB is a NW–SE oriented, elongated sedimentary unit situated on the Lower Paleozoic metamorphic basement. The basin comprises a variety of volcanic and sedimentary rocks dating back to the Upper Carboniferous, Permian, Triassic and Cretaceous (Głuszyński and Aleksandrowski, 2022). Permian rocks include mainly Rotliegend and Zechstein strata (Milewicz, 1985; Raczyński, 2010). The study area is situated in the marginal part of the ancient Zechstein Sea Basin, which changed its extent over time due to periodical transgressions and regressions. This resulted in the deposition of continental and shallow marine sediments, now comprising marls, dolomites, sandstones, and limestones, which are referred to as consecutive cyclothems. This area has undergone significant folding and faulting, primarily during the Cretaceous Period when Variscan fault zones were re-activated during the Alpine orogeny (Głuszyński and Aleksandrowski, 2022). Towards the end of the Cretaceous and the climax of the orogenic movements, the basin was tectonically inverted and uplifted because of compressional deformation (Leszczyński and Nemec, 2019) to be further eroded to the approximately current configuration.

Mineralization in the area began in the Triassic, driven by interactions between oxidized saline brines and the reduced organic-rich Kupferschiefer shales (Alderton et al., 2016). Copper deposits, primarily composed of malachite along with minor amounts sulphides such as covellite, chalcopyrite and pyrite (Oszczepalski, 1999), are found near the margins of the NSB within the Zechstein Limestone (Ca1). Shallow ore deposits facilitated early mining in the region.

HISTORICAL SETTING

Since the medieval and early modern periods, the OCB region developed a long history of mining and smelting activities centred around copper. Mining traces date back to the 13th century, with more structured efforts appearing by the 15th century, particularly around Złotoryja town and the Leszczyna Basin (Fig. 1B). Copper ore extraction was difficult due to the modest ore quality and small deposits, resulting in numerous short-lived operations. The 17th and 18th centuries saw some successes, with mines such as Character and Leszczyńska, and a prominent smelting centre, Stilles Glück, which operated intermittently from the mid-1800s. Smelting remains provide evidence for differing furnace designs over the centuries, hinting at changing technologies and varying production temperatures (more on these topics: Kądziołka et al., 2020; Derkowska et al., 2021). Mining efforts in the area saw a resurgence in the mid-20th century, marked by the Lena mine's operations. Currently the area is not considered to be profitable for copper extraction.

MATERIALS AND METHODS

MATERIALS

Soil samples were systematically collected in 2016–2017 near historical mining sites in Leszczyna and Kondratów (Fig. 1B). In total, 38 soil samples (22 topsoil, 16 subsoil), 10 rock samples, and 10 slag samples were selected for this study.

Topsoils were collected from different land-use areas, including historical mining and smelting zones in Leszczyna (SOK4–SOK9) and Kondratów (SOK20, SOK21; Fig. 1C, D). Additional background topsoils were acquired from the northern (SOK1, SOK2, SOK18, SOK19) and eastern (SOK3) surroundings of the site. Topsoils were generally taken from the upper 0–10 cm, unless the organic layer was thicker or thinner. Each soil sample represents a composite collected from the midpoint of the respective horizon, and the exact sampling depths for all horizons are provided in Table 1. Soil profiles were also established in the immediate vicinity of the historical smelting area (Fig. 1D), with two (PL1 and PL2) serving as representative of background geochemical conditions based on their distance from smelting features and low metal concentrations, while the remaining four (PL3, PL4, PL5, and PL6) show varying degrees of anthropogenic influence. For each soil horizon, a sample of approximately 300-600 grams was extracted from the midpoint of the horizon, contingent on its thickness. Following acquisition, soil samples were air-dried until cessation of mass change, and sieved to 2 mm with a laboratory sieve. The <2 mm fraction was subsequently pulverized and used for chemical and isotopic analyses.

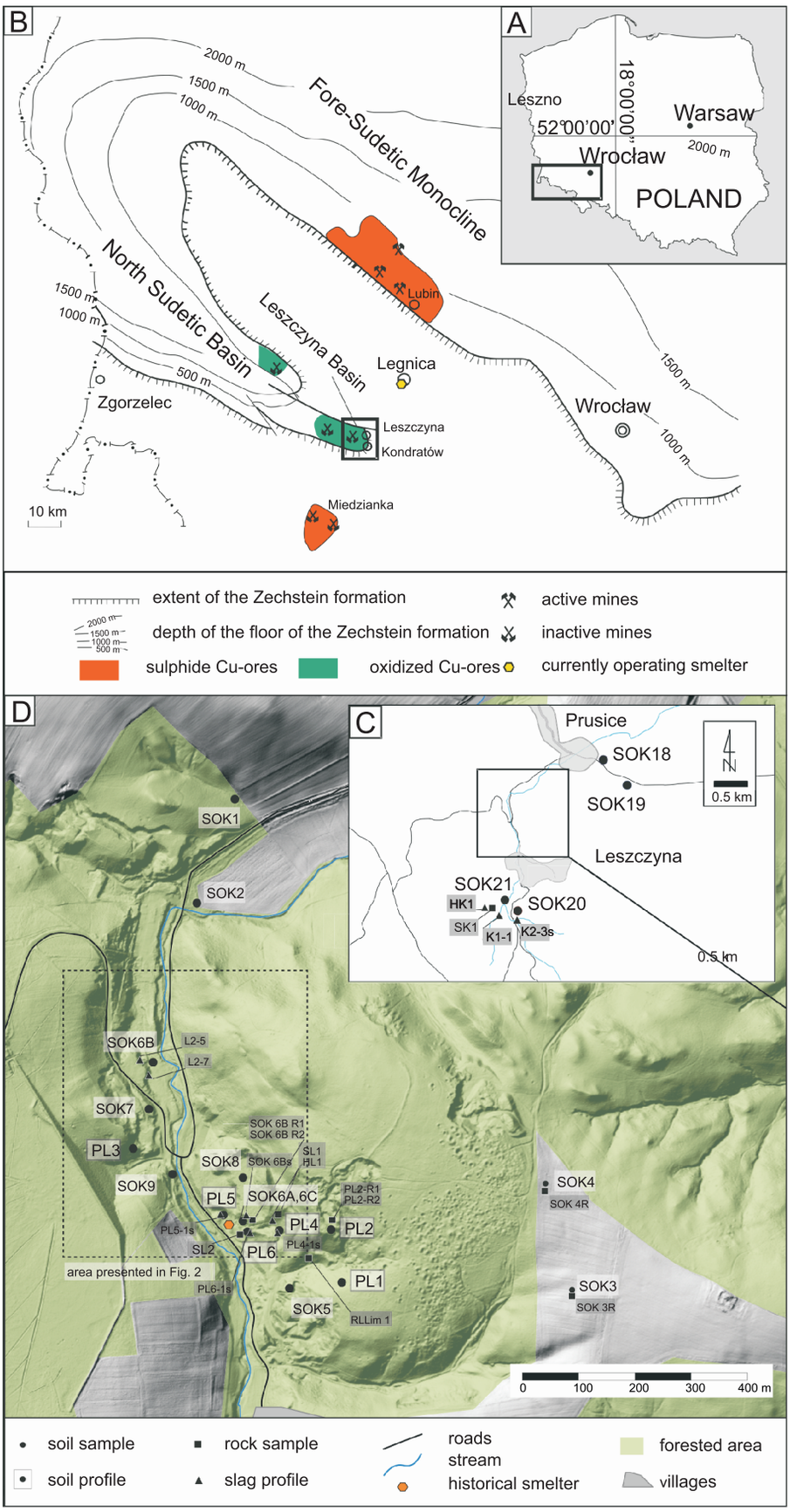

Fig. 1. Location of copper ore deposits and mining districts in south-western Poland with an approximate extent and depth of the Zechstein Formation within the Fore-Sudetic Monocline and the North Sudetic Basin (A, B) and research site near Leszczyna with detailed sampling sites (C, D)

B – modified after Stolarczyk et al. (2015), D – modified after Derkowska et al. (2023)

Table 1

Elemental (mg kg^{-1}) and Pb isotopic (^{206}Pb/^{207}Pb, ^{208}Pb/^{206}Pb) compositions in soils together with the Pb isotopic results for the EDTA extracts

		Depth (cm)	Cu	Pb	Th	U	U/Pb	Th/Pb	^{206}Pb/^{207}Pb	SD	^{208}Pb/^{206}Pb	SD	EDTA ^{206}Pb/^{207}Pb	SD	EDTA ^{208}Pb/^{206}Pb	SD
topsoil	SOK1	0–10	125	68	14	1	0.0	0.2	**1.180**	0.006	**2.088**	0.006	**1.187**	0.008	**2.061**	0.016
	SOK3	0–10	62	39	6	2	0.0	0.2	**1.177**	0.006	**2.083**	0.005	**1.176**	0.012	**2.088**	0.019
	SOK5	0–10	256	58	5	4	0.1	0.1	**1.187**	0.003	**2.070**	0.007	**1.177**	0.011	**2.099**	0.026
	SOK7	0–10	99	47	9	3	0.1	0.2	**1.177**	0.003	**2.087**	0.006	nd	nd	nd	nd
	SOK8	0–10	329	57	8	3	0.1	0.1	**1.191**	0.003	**2.059**	0.004	**1.174**	0.006	**2.085**	0.01
	SOK18	0–10	nd	nd	nd	nd	nd	nd	**1.196**	0.002	**2.084**	0.003	**1.184**	0.009	**2.081**	0.017
	SOK19	0–10	nd	nd	nd	nd	nd	nd	**1.193**	0.002	**2.085**	0.003	**1.182**	0.007	**2.065**	0.008
	PL1 A	0–13	103	71	22	3	0.0	0.3	**1.175**	0.005	**2.097**	0.011	**1.158**	0.007	**2.097**	0.022
	PL3 A	0–10	120	50	11	3	0.1	0.2	**1.172**	0.008	**2.096**	0.005	**1.177**	0.016	**2.085**	0.013
	SOK2	0–10	2139	555	11	13	0.0	0.0	**1.181**	0.008	**2.088**	0.012	**1.181**	0.006	**2.076**	0.009
	SOK4	0–10	1076	43	9	4	0.1	0.2	**1.214**	0.006	**2.018**	0.012	**1.196**	0.009	**2.062**	0.012
	SOK6 A	0–10	2181	140	5	4	0.0	0.0	**1.175**	0.004	**2.090**	0.007	**1.176**	0.01	**2.103**	0.022
	SOK6 B	0–10	4705	145	9	10	0.1	0.1	**1.185**	0.000	**2.077**	0.003	**1.182**	0.011	**2.084**	0.018
	SOK6 C	0–10	2199	78	7	4	0.0	0.1	**1.184**	0.006	**2.076**	0.007	nd	nd	nd	nd
	SOK9	0–10	981	66	8	4	0.1	0.1	**1.184**	0.002	**2.077**	0.001	**1.164**	0.012	**2.094**	0.013
	PL2 O	0–5	453	219	3	2	0.0	0.0	**1.173**	0.003	**2.095**	0.005	**1.180**	0.02	**2.076**	0.01
	PL5 A1	0–5	835	123	8	4	0.0	0.1	**1.181**	0.002	**2.079**	0.004	**1.177**	0.016	**2.094**	0.024
	PL6 O	0–12	592	281	3	3	0.0	0.0	**1.174**	0.002	**2.089**	0.005	**1.179**	0.015	**2.087**	0.028
	SOK20	0–10	nd	nd	nd	nd	nd	nd	**1.189**	0.002	**2.098**	0.003	**1.212**	0.01	**2.03**	0.017
	SOK21	0–10	nd	nd	nd	nd	nd	nd	**1.260**	0.002	**1.988**	0.003	**1.181**	0.015	**2.081**	0.017
	PL4 A1	0–15	860	50	5	3	0.1	0.1	**1.180**	0.003	**2.068**	0.005	**1.189**	0.012	**2.086**	0.011
subsoil	PL1 B	13–35	22	25	16	2	0.1	0.6	**1.184**	0.002	**2.093**	0.007	**1.182**	0.005	**2.081**	0.01
	PL1 C	35–80	11	24	19	3	0.1	0.8	**1.201**	0.001	**2.088**	0.005	**1.182**	0.011	**2.08**	0.009
	PL2 C1	5–25	1378	81	17	18	0.2	0.2	**1.234**	0.004	**1.993**	0.005	**1.228**	0.02	**1.997**	0.01
	PL2 C2	25–40	1300	29	7	5	0.2	0.3	**1.223**	0.003	**2.001**	0.004	**1.177**	0.022	**2.064**	0.019
	PL3 B	10–25	17	16	10	2	0.1	0.6	**1.194**	0.004	**2.072**	0.005	**1.202**	0.008	**2.075**	0.009
	PL3 C	25–50	12	19	13	3	0.1	0.7	**1.189**	0.001	**2.076**	0.006	nd	nd	nd	nd
	PL4 A2	15–60	827	42	4	3	0.1	0.1	**1.189**	0.005	**2.061**	0.007	**1.194**	0.007	**2.051**	0.023
	PL4 B	60–90	1154	171	2	1	0.0	0.0	**1.190**	0.002	**2.057**	0.007	**1.183**	0.014	**2.077**	0.02
	PL5 A2	5–10	1163	85	10	5	0.1	0.1	**1.185**	0.003	**2.068**	0.007	**1.174**	0.004	**2.08**	0.026
	PL5 B	10–100	84	25	11	3	0.1	0.4	**1.199**	0.002	**2.064**	0.008	**1.194**	0.004	**2.056**	0.026
	PL5 B40	40	142	26	10	2	0.1	0.4	**1.195**	0.002	**2.079**	0.005	nd	nd	nd	nd
	PL5 B60	60	73	24	11	3	0.1	0.4	**1.197**	0.004	**2.078**	0.007	nd	nd	nd	nd
	PL5 B80	80	55	24	11	3	0.1	0.4	**1.201**	0.004	**2.058**	0.006	nd	nd	nd	nd
	PL5 B100	100	54	23	13	4	0.2	0.6	**1.207**	0.003	**2.057**	0.004	nd	nd	nd	nd
	PL6 A	12–47	2734	88	7	12	0.1	0.1	**1.228**	0.003	**1.998**	0.009	**1.188**	0.005	**2.06**	0.019
	PL6 B	47–82	6920	143	14	14	0.1	0.1	**1.198**	0.004	**2.045**	0.006	**1.195**	0.007	**2.048**	0.012
	PL6 C2	82–94	904	27	5	5	0.2	0.2	**1.183**	0.002	**2.079**	0.005	**1.194**	0.004	**2.059**	0.021

nd – not determined (the dataset reported by Derkowska et al., 2023, excluding the U/Pb, Th/Pb and isotopic parameters)

Rock and slag samples were characterized in detail by Derkowska et al. (2023). Here we summarize only aspects relevant to Pb isotopes. The rock samples collected include both ore-bearing and surrounding host lithologies representative of the local geology. Among the non-mineralized or weakly mineralized types are slates and limestones (Table 2) as well as one phyllite sample from the Kaczawa Metamorphic Complex, all displaying minimal Cu content. In contrast, several samples show notable mineralization typical of the Zechstein Limestone (Ca1; Table 2).

Slags were collected from the surrounding of the smelting and mining area where they are located primarily in waste piles (WP; Fig. 2) and additionally around the area within the soil surface (Fig. 1D). Ten samples were analysed (Table 2) to determine their lead isotopic composition, serving as a smelting Pb isotopic signal. The slags are typically glassy, porous, and dark grey to black (more in: Kądziołka et al., 2019, 2020). Their size varies notably, from small, irregular fragments (3–10 cm) to large, angular blocks (up to 20 20 20 cm). Rocks and slags were carefully cleaned under running water and dried at room temperature, and then divided into two parts: a subsample intended for thin section preparation and the remaining part, which was crushed and pulverized.

CHEMICAL ANALYSES

Whole-rock major and trace element geochemistry and mineral compositions determined by EPMA were reported previously (Derkowska et al., 2023). However, given the nature of the isotopic analyses, we provide more details on chemical analyses.

Major, minor and trace elements were analysed in the Institute of Geochemistry, Mineralogy and Mineral Resources laboratory at Charles University, Prague. Samples (100–200 g, depending on the original size) were milled using an agate pulverizer ring mill and 0.2 g was dissolved in 10 mL of HF (49% v/v) and 0.5 mL of $HClO_4$ (70% v/v). Samples were later dried for 2.5 h at 150°C and the procedure was repeated using 5 mL

Table 2

Elemental (mg kg^{-1}) and Pb isotope compositions in rock and slag

	Sample	Characteristics	Cu	Pb	Th	U	U/ Pb	Th/Pb	$^{206}Pb/^{207}Pb$	SD	$^{208}Pb/^{206}Pb$	SD
Rock	PL2-1 R1	slate	20980	47	8	24	0.5	0.2	**1.261**	0.004	**1.943**	0.007
	PL2-1 R2	slate	5280	10	3	19	1.8	0.3	**1.448**	0.002	**1.675**	0.002
	SL1	slate	4421	28	1	12	0.4	0.0	**1.246**	0.006	**1.972**	0.007
	SK1	dolomite	10490	7	8	23	3.4	1.2	**1.766**	0.008	**1.370**	0.003
	RLLim 1	limestone	4445	8	2	18	2.3	0.3	**1.536**	0.002	**1.567**	0.004
	SOK6B R1	marl	1165	10	1	6	0.6	0.1	**1.260**	0.002	**1.943**	0.005
	SL2	slate	55	44	2	1	0.0	0.0	**1.192**	0.005	**2.063**	0.008
	SOK6B R2	slate	132	29	1	2	0.1	0.0	**1.169**	0.003	**2.087**	0.006
	SOK4R	limestone	149	21	2	13	0.6	0.1	**1.284**	0.005	**1.911**	0.004
	SOK3R	phyllite	32	11	2	bdl	0.0	0.2	**1.181**	0.003	**2.086**	0.004
Slag	HL1	intermediate	3941	46	14	38	0.8	0.3	**1.182**	0.002	**2.070**	0.002
	PL4-1s A	intermediate	3206	21	16	54	2.6	0.8	**1.240**	0.002	**1.972**	0.004
	PL5-1s A	intermediate	1400	5	16	41	8.2	3.3	**1.151**	0.002	**2.079**	0.004
	PL6-1s	intermediate	2156	2	15	46	23.0	7.7	**1.209**	0.003	**2.017**	0.004
	SOK 6Bs	intermediate	1745	10	nd	nd	nd	nd	**1.209**	0.002	**2.023**	0.004
	K2-3	intermediate	1874	6	15	34	6.3	2.6	**1.228**	0.003	**1.993**	0.005
	L2-5	young	5162	83	13	49	0.6	0.2	**1.174**	0.001	**2.082**	0.002
	L2-7	young	3097	128	11	48	0.4	0.1	**1.165**	0.002	**2.092**	0.003
	HK1	old	73185	46	12	27	0.6	0.3	**1.188**	0.001	**2.071**	0.003
	K1-1	old	72595	9	15	66	7.4	1.7	**1.209**	0.003	**2.024**	0.005

nd – not determined, bdl – below detection limit. Grey background – determined in the isotope laboratory in Prague, white background – determined in the BVM lab (the dataset reported by Derkowska et al., 2023, excluding the U/Pb, Th/Pb and isotopic parameters)

of 40% HF with 1 mL $HClO_4$. The residue was dissolved in 2 mL HNO_3, filtered, and diluted to 100 mL using deionized ultrapure water. The filter was additionally burned with 0.5 g of soda and borax flux, melted, and digested in 2% HNO_3 and added to the filtered solution to 100 mL. All the acids used in the dissolution procedure were reagent grade (Merck, Germany) and double distilled. MilliQ+ deionized water obtained from a Millipore system was used for dilution. The total content of Cu, Ni, Pb, Zn, Cr and As was analysed with inductively coupled plasma optical emission spectrometry (ICP-OES, Thermo Scientific iCAP 6500, Germany) and quadrupole-based inductively coupled plasma mass spectrometry (ICP-MS, X Series 2, Thermo Scientific) under standard analytical conditions (described in detail in Mihaljevič et al., 2011). The analytical reproducibility (2) reached approx. 2.20% for major elements and av. 1.73% for minor elements and was estimated with six replicate sample analyses. The analytical accuracy (2) was determined using two certified standards, including NIST 2782 and SU-1b. The results reached 1.78% for major and av. 8.83% for minor elements.

Soil samples were additionally subjected to EDTA extraction following Quevauviller (1998). The elemental composition of the leachates has been described elsewhere (Derkowska et al., 2023). Here, these leachates were further analysed for Pb isotopes, as described below.

ISOTOPE ANALYSES

Bulk Pb concentrations were first established, after which dissolved samples were diluted with 2% (v/v) HNO_3 to obtain 20–25 μg L^{-1} total Pb for isotopic analysis. Lead isotopes (^{206}Pb, ^{207}Pb, ^{208}Pb) were measured using a quadrupole-based inductively coupled plasma mass spectrometer (ICP-MS, X Series 2, Thermo Scientific) at the Institute of Geochemistry, Mineralogy and Mineral Resources, Charles University, Prague, following analytical conditions described by Mihaljevič et al. (2011). Each sample was analysed five times, and mean values were corrected using interspersed standard measurements. Mass bias was corrected with NIST 981, analysed between every two samples. Standard reference materials (NIST 2782, BCR 2) were included for quality control. Reproducibility reached up to 3.9% (median: 1.8%) based on replicate analyses of six samples. Standard deviations for isotope ratios were up to 4.90% for slag, 1.71% for rock, and 2.09% for soil samples.

RESULTS

BACKGROUND FROM PREVIOUS RESEARCH: SOIL, ROCK AND SLAG COMPOSITION WITH FOCUS ON LEAD DISTRIBUTION

The textures, physicochemical properties and bulk geochemistry of the soils studied were previously characterized by Derkowska et al. (2023) and are briefly summarized here to provide context for Pb isotope analyses. The topsoils are typically silt loams and subsoil sandy loams, with pH values ranging from slightly acidic to neutral (5.6–7.3). Organic matter is concentrated in the upper horizons.

The major element composition of soils is dominated by SiO_2 (49 wt.% in topsoils, 62 wt.% in subsoils), with Al_2O_3, Fe_2O_3, K_2O, MgO, and CaO contributing 1–11 wt.% each (Derkowska et al., 2023, SM7). Trace elements reveal strong enrichment in metals associated with historical mining and smelting, including Cu (up to 6920 mg kg^{-1}), Ni (up to 340 mg kg^{-1}), As (up to 130 mg kg^{-1}), Zn (up to 400 mg kg^{-1}), and finally Pb (up to 555 mg kg^{-1}; Fig. 2). Most of these metal(loid)s are concentrated in organic-rich topsoils near a stream-adjacent plateau. Lead, however, displays a distinct distribution: unlike Cu, Zn, Ni and As, which remain localized near former industrial areas, especially WP1, Pb enrichment extends northwards beyond the mining boundaries (Fig. 2). This pattern suggests an additional source of the element and provides the framework for the Pb isotope study described below.

Differences between Pb and other metal(loid)s are also evident in vertical soil profiles. Copper concentrations are highly variable, ranging from 62 to 4705 mg kg^{-1} in topsoils (median 592 mg kg^{-1}) and 11 to 6920 mg kg^{-1} in subsoils (median 142 mg kg^{-1}; Table 1). By contrast, Pb concentrations are lower and more surface-confined, with 39–555 mg kg^{-1} in topsoils and 16–171 mg kg^{-1} in subsoils (medians 68 and 26 mg kg^{-1},

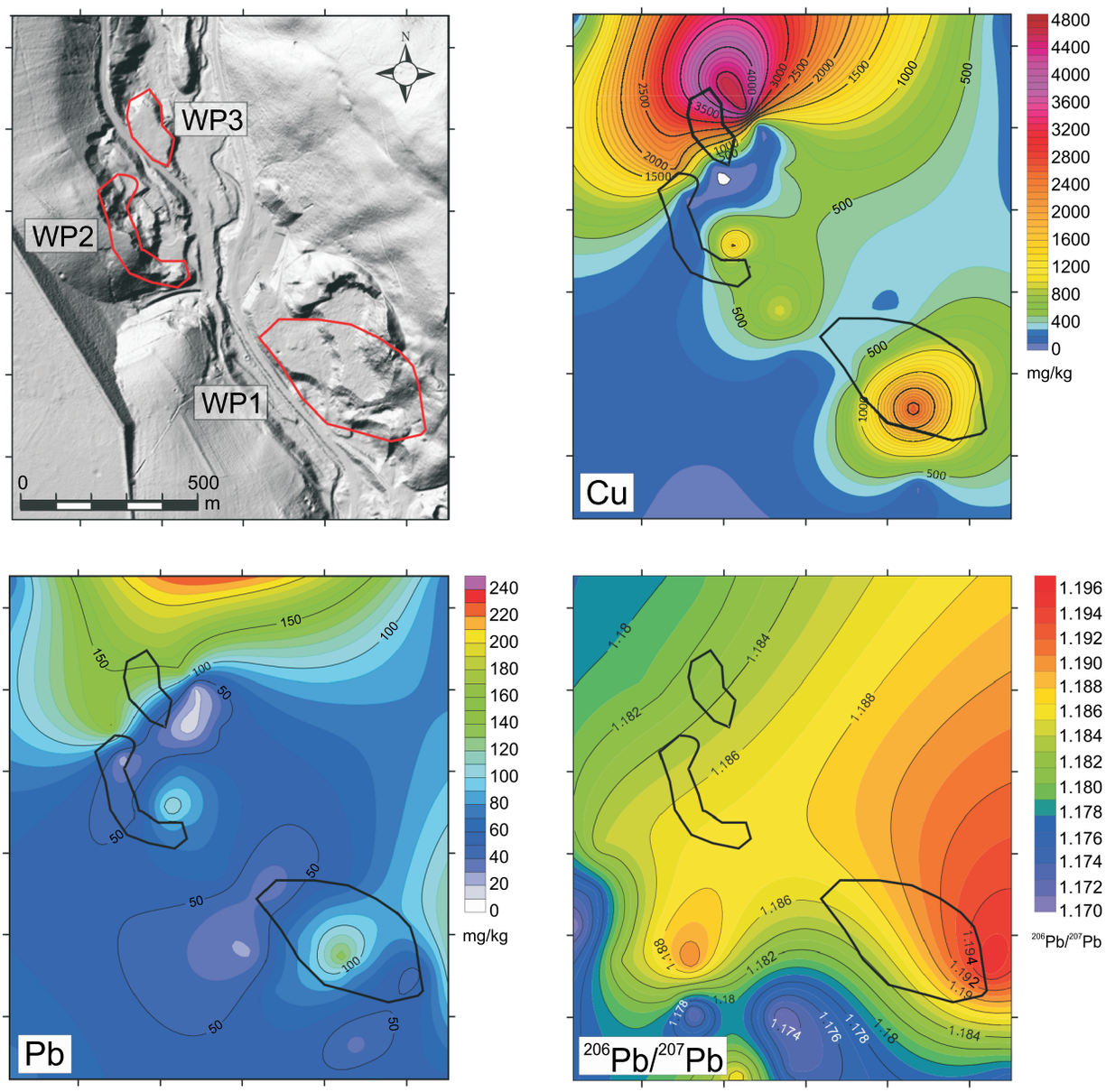

Fig. 2. Spatial distribution of Cu, Pb and ^{206}Pb/^{207}Pb ratios in soils of the research area

Black outlines mark historical waste piles (modified after Derkowska et al., 2023)

respectively; Fig. 3). This disparity suggests Pb contamination is predominantly surface-derived, whereas Cu maxima may occur either at the surface or at depth, depending on local geology and proximity to ore-bearing rocks or smelting residues. Although both elements exceed global background levels (Pb ~27 mg kg^{-1}, Cu ~14 mg kg^{-1}; Kabata-Pendias and Szteke, 2015), Pb contamination remains moderate relative to Cu enrichment.

The rocks have generally low Pb contents (6–47 mg kg^{-1}; Table 2). Slag samples are chemically heterogeneous and enriched in Cu, but they also contain measurable Pb (up to 128 mg kg^{-1}; Table 2). These materials represent potential sources of Pb in soils and are revisited in the isotopic discussion below. Taken together, the soil, rock and slag compositions establish the geochemical background against which Pb isotope data can be evaluated.

SUBSOIL TEXTURAL CHARACTERISTICS

Profiles PL1 and PL2, located in the southeastern part of the site (Fig. 1), represent natural soils. PL1, developed on unmineralized sandstone, shows a typical sequence of organic (O), leached (A), clay-rich (B), and parent material (C) horizons, reaching sandstone bedrock at ~60 cm depth (Fig. 4). PL2, formed on Cu-enriched marl (Fig. 1), is shallower (~37 cm) and displays colour variations reflecting mineralogical contributions from the Cu-bearing substrate. In contrast, profiles PL3–PL6 show varying degrees of anthropogenic modification (Fig. 4). PL3, located on a waste heap, retains elements of a natural sequence but contains minor slag inclusions and compacted horizons with reduced biological activity. PL4, located below a slag wall, is strongly disturbed, with irregular horizons composed of mixed organic and mineral materials, likely influenced by leach-

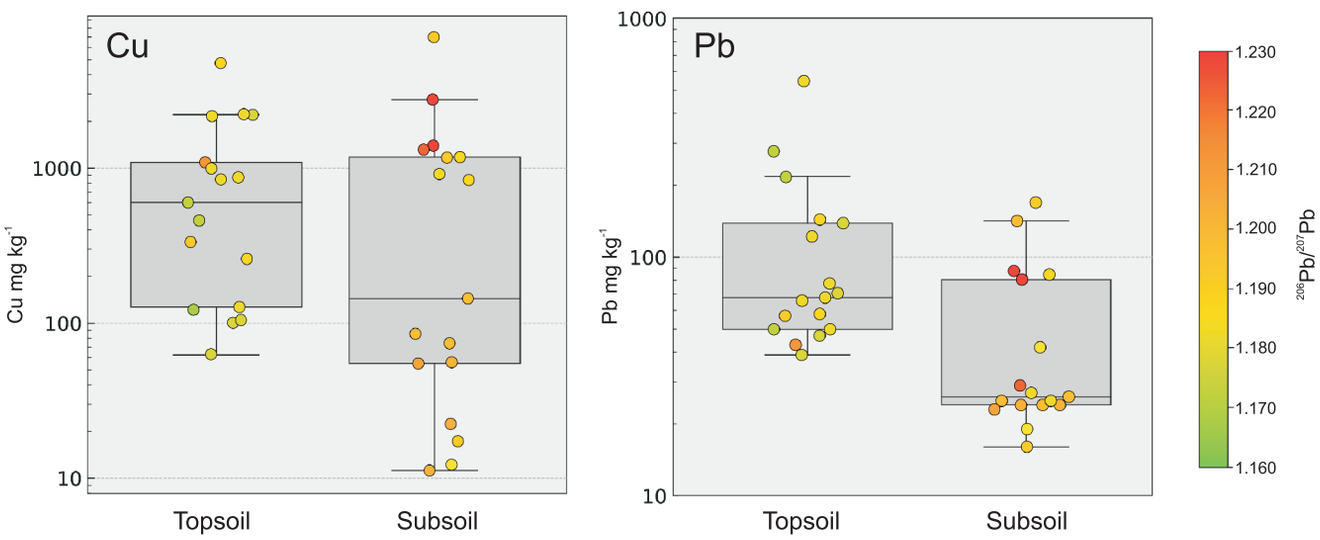

Fig. 3. Boxplots of Cu and Pb concentrations in topsoil and subsoil samples from the Leszczyna area

Individual data points are colour-coded by $^{206}Pb/^{207}Pb$ isotope ratios, illustrating metal enrichment and isotopic variability between soil horizons

ing from overlying slag. PL5, located near the smelter, is the deepest (up to 120 cm) and shows relatively stable loamy textures, though shallow horizons contain minor slag fragments. PL6, situated beneath a former waste pile, is the most disrupted: horizons are obliterated, and the profile is intermixed with slag, tailings and lithological debris, preventing natural soil development (Fig. 4). Together, the profiles illustrate a gradient from natural pedogenesis (PL1–PL2) to severe post-industrial alteration (PL6). This vertical perspective complements the bulk soil data and provides additional context for interpreting Pb distribution and isotopic signatures.

LEAD ISOTOPIC COMPOSITION

TOPSOILS

Topsoil samples (0–15 cm) show a relatively narrow but distinct range of $^{206}Pb/^{207}Pb$ ratios, typically between 1.172 and 1.196, with most values clustering around 1.172–1.185 (Table 1). These isotopic signatures are generally associated with elevated Pb concentrations (commonly 50–150 mg kg^{-1}) and, in many cases, high Cu levels (commonly >500 mg kg^{-1}; Fig. 3). Some of these samples are strongly enriched in Cu (ranging from ~800 to over 4700 mg kg^{-1}; Table 1), likely reflecting the legacy of local ore processing or deposition of metallurgical residues (Derkowska et al., 2023). Despite these high metal loads, their isotopic ratios cluster around $^{206}Pb/^{207}Pb$ 1.18. A few topsoil samples deviate from this pattern. For example, SOK4 and PL6 A show more radiogenic values (1.214 and 1.228, respectively), which may reflect localized input from weathered ore or slag materials rather than regional contamination.

Because of the limited isotopic diversity in the topsoils, the spatial distribution of $^{206}Pb/^{207}Pb$ ratios shows a relatively consistent pattern throughout much of the study area, with most samples – particularly those from the central and western zones – falling within a narrow range of 1.172 to 1.185 (Table 1 and Fig. 2). These samples are broadly distributed and not confined to any single landform or soil type.

Slightly elevated isotopic ratios are observed in SOK21 (1.260), SOK4 (1.214), SOK18 (1.196), and SOK19 (1.193), which are located in the southern and eastern parts of the study area, away from the core of historical smelting operations (Fig. 1). These differences occur regardless of visible smelting remnants or mineral exposures and extend across valleys, slopes and upper terraces, suggesting a complex spatial pattern. Lower isotope ratios are not restricted to areas near metallurgical waste, while more radiogenic signatures appear at scattered, commonly peripheral, locations (Fig. 2).

SUBSOIL

Subsoils (n = 17), in contrast to topsoils, display broader isotopic variability, with $^{206}Pb/^{207}Pb$ ratios ranging from 1.183 to 1.234 (Table 1). Many soil profiles show a systematic increase in the lead isotopic ratio with depth, particularly evident in natural profiles, i.e., PL1 and PL2 (Fig. 4). For example, PL2 shows a distinct upwards trend in $^{206}Pb/^{207}Pb$ from 1.173 at the surface to 1.234 at the base. This suggests that deeper soil horizons retain a lithogenic or ore-related isotopic signal that is distinct from the topsoil's isotopic signal.

EDTA SOIL LEACHATE ISOTOPIC BEHAVIOUR

Analysis of EDTA-extractable Pb further exemplifies the behaviour of the mobile lead fractions. The EDTA-extractable $^{206}Pb/^{207}Pb$ ratios across the soils studied range from 1.158 to 1.228, with most values clustering between 1.17 and 1.19 (Table 1). This narrow range is particularly evident in topsoil samples (typically 0–10 cm), suggesting a relatively homogeneous isotopic signature for the mobile lead fraction in surface horizons. In subsoils the EDTA-extractable Pb shows a broader isotopic spread, with values ranging from 1.228 (e.g., PL2 C1) to 1.174 (e.g., SOK8). Several profiles also show vertical changes in EDTA-extractable isotopic ratios, such as PL6, where values shift from 1.188 (horizon A) to 1.195 (horizon B), and 1.194 (horizon C2).

Within the dataset, 20 out of 31 analysed samples showed lower $^{206}Pb/^{207}Pb$ values in the EDTA-leachable fraction compared to the bulk data, typically by 0.008–0.015. This trend is consistent in both topsoils and subsoils, although in subsoils it reaches 75% compared to 57% in topsoils. Topsoils, on the other hand, show a broader range of differences, including the largest observed decrease of ~0.079 and increase of 0.070.

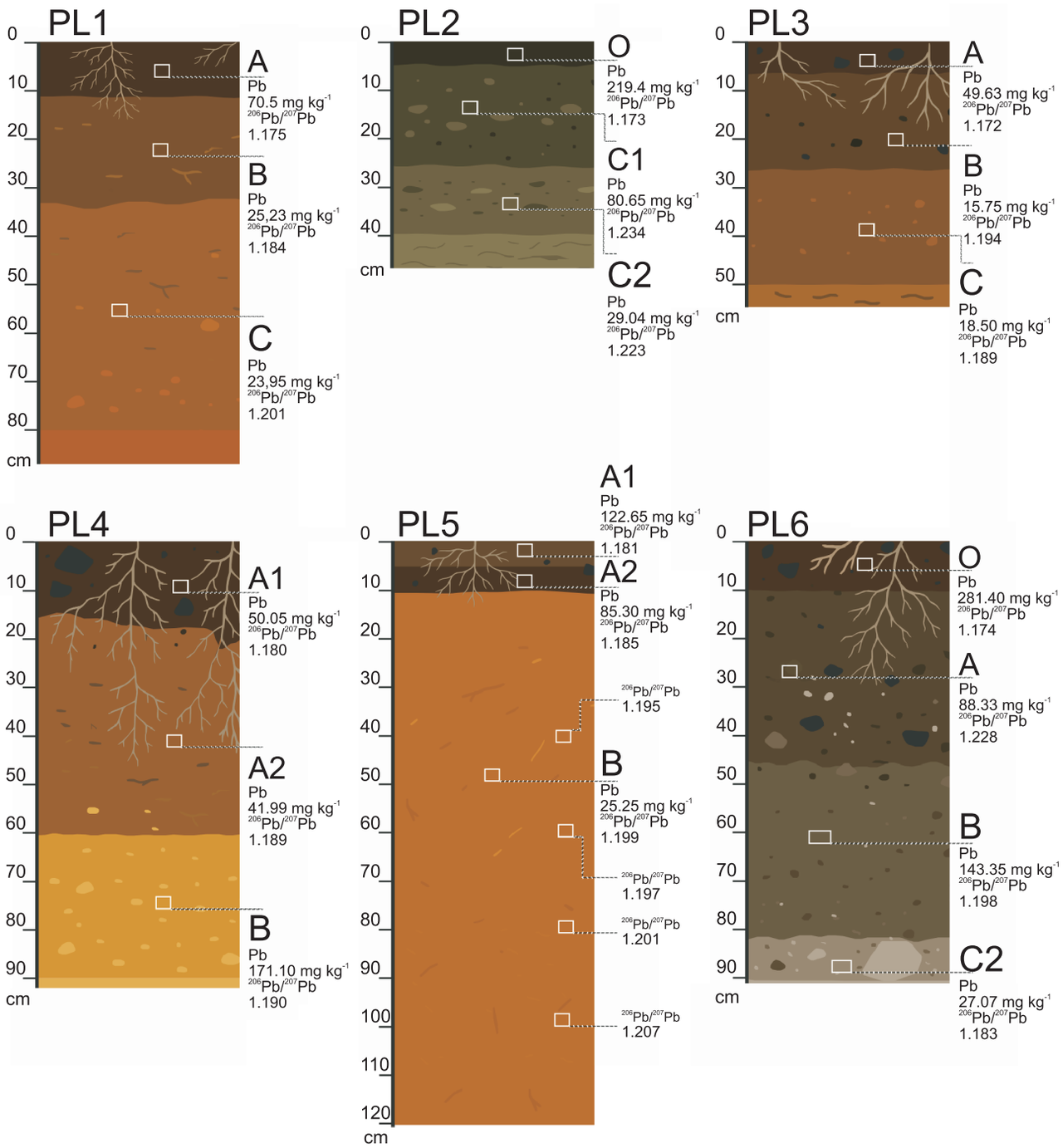

Fig. 4. Soil profiles (PL1–PL6) showing Pb concentrations (mg kg^{-1}) and corresponding $^{206}Pb/^{207}Pb$ isotope ratios with depth

Horizons (O, A, B, C) are indicated; white squares mark sampling positions. Profiles PL1–PL3 – naturally developed soil profiles (PL2 – developed on Cu-rich slates), PL4–PL6 – anthropogenically impacted profiles

Nine samples showed higher EDTA-leachable ratios (generally up to ~0.02), mainly in topsoils, and one sample displayed the same isotopic values in both EDTA and bulk.

This suggests that the EDTA-extractable fraction is generally less radiogenic than bulk Pb, indicating isotopic differentiation between mobile and total Pb pools. In all samples, the bulk–EDTA offsets span –0.079 to +0.070, encompassing both the typical small differences and the few more pronounced deviations. Most samples fall within ±0.02 (less than ±0.015 for subsoils). This suggests that while there is a general trend of isotopically less radiogenic EDTA-leachable Pb, the degree of this offset can vary, likely reflecting differences in source contributions, Pb speciation, or soil chemistry.

LOCAL LEAD SOURCES

Although lead concentrations in the rocks are relatively low (6–47 mg kg^{-1}), Pb isotopic signatures display substantial variability. Some rocks, such as limestones and slates with limited mineralization (e.g., SOK6B R2, SL2), show less radiogenic

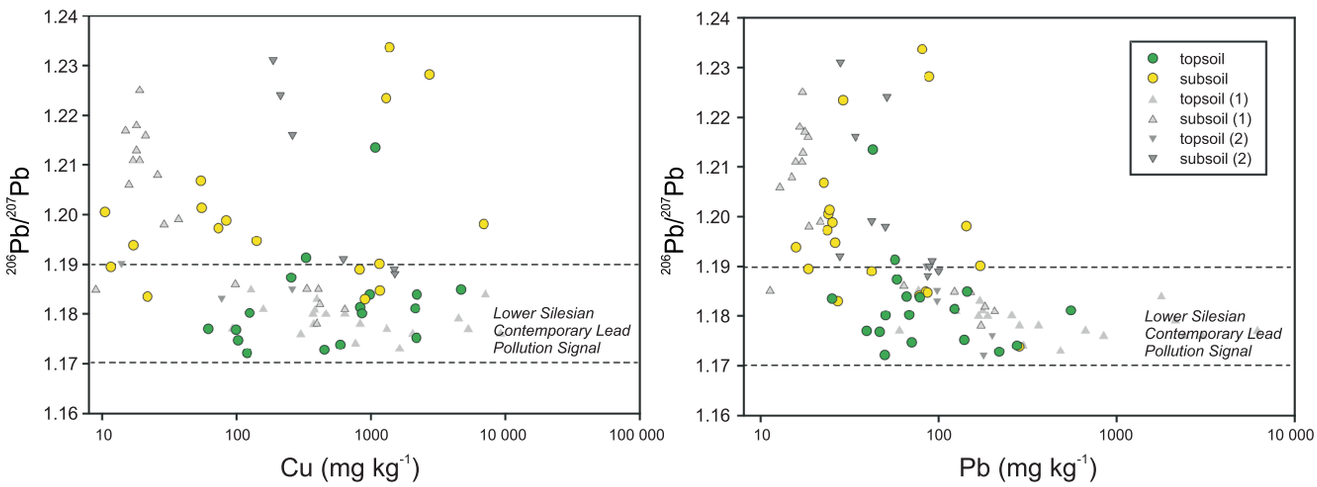

Fig. 5. $^{206}Pb/^{207}Pb$ ratios as a function of total Cu and Pb concentrations as measured for topsoil and subsoil samples compared to topsoils from other studies in the same region after Tyszka et al. (2012); Kierczak et al. (2013)

$^{206}Pb/^{207}Pb$ ratios (1.169–1.192; Table 2), overlapping with values observed in upper soil horizons. In contrast, certain dolomites and mineralized slates show highly radiogenic signatures (up to 1.766), likely reflecting prolonged geogenic evolution (though this is not the focus of this article). Differences are evident between Cu-mineralized and unmineralized rocks. Unmineralized rocks tend to have less radiogenic $^{206}Pb/^{207}Pb$ ratios (1.169–1.284; Table 2), whereas Cu-rich rocks display a wider range (1.246–1.766) and higher median U contents (19 mg kg^{-1} *versus* 2 mg kg^{-1} in unmineralized samples).

Slag samples also show variability in Pb isotopes, although smaller than in the rocks. The most radiogenic slag reaches a $^{206}Pb/^{207}Pb$ ratio of 1.240. Age-dependent trends are observed: the oldest slags (HK1, K1-1) present narrow ratios (1.188–1.209), as do the youngest (L2-5, L2-7: 1.165–1.174). Intermediate-age slags show greater variation, with ratios spanning 1.151–1.240 (Table 2). This pattern likely reflects both the larger number of intermediate-age samples and historical smelter activity (Kądziołka et al., 2020): during peak production at the Stilles Gluck smelter, mixed ores (shale and marl) were used, producing slags with more variable chemical and isotopic compositions. In contrast, older and younger slags were produced from more homogeneous ore, resulting in narrower isotopic ranges.

DISCUSSION

LEAD IN THE RESEARCH AREA

The isotopic composition of lead in the topsoils studied reflects the interplay of multiple Pb sources, including local lithogenic contributions, legacy metallurgical inputs, and atmospheric deposition, as has been demonstrated in numerous studies (Tyszka et al., 2012; Komárek et al., 2008). Most topsoil samples showed relatively low and tightly clustered $^{206}Pb/^{207}Pb$ ratios (1.172–1.185). Notably, this isotopic range is observed consistently across different surface environments within the study area, i.e., including zones not directly influenced by historical mining or smelting, indicating that neither lithogenic nor metallurgical sources alone can explain the uniformity observed. Considering the homogeneity of Pb isotopic signal in the topsoils, combined with elevated Pb concentrations and lower $^{206}Pb/^{207}Pb$ ratios (Fig. 5) we suggest that Pb in the topsoils is predominantly derived from atmospheric deposition. Similar homogenized signatures attributed to long-range atmospheric deposition have been reported in other Central European settings (Reimann et al., 2012; Tyszka et al., 2012; Fiałkiewicz-Kozieł et al., 2020).

The subsoils reveal a broader and systematically higher range of $^{206}Pb/^{207}Pb$ ratios, from 1.183 up to 1.234 (Fig. 5), with values increasing with depth in several profiles (Table 2 and Fig. 4). This suggests the presence of a lithogenic Pb component, potentially derived from local bedrock or mineralization (see next section). Comparable vertical contrasts between isotopically less radiogenic topsoils and more radiogenic subsoils are characteristic of soils where lithogenic Pb persists at depth while atmospheric inputs dominate surface layers (Sipos et al., 2013). A comparison between Pb isotopic composition and Cu concentrations further supports these observations. Topsoil samples with lower Cu concentrations tend to show lower $^{206}Pb/^{207}Pb$ ratios than Cu-enriched soils. Similarly, in subsoils, higher Cu levels are commonly associated with higher Pb isotope ratios, reflecting the influence of ore-hosting lithologies. These observations suggest distinct Pb sources in the topsoils and subsoils within the study area, with rocks and/or slags representing low-Pb, isotopically more radiogenic endmembers.

EDTA-extracted Pb supports this vertical trend. Topsoils contain more mobile Pb with less radiogenic isotopic ratios, while subsoils retain less labile, isotopically more radiogenic Pb (Table 1; Derkowska et al., 2023). This behavior aligns with studies showing that anthropogenic Pb tends to be concentrated in the exchangeable fraction of surface soils, while lithogenic Pb dominates more immobile pools at depth (Komárek et al., 2008). Collectively, these data indicate a decoupling of modern pollution from geological Pb sources. This shift, from relatively unpolluted older materials to polluted modern ones, is also observed in diverse sedimentary records, including the nearby Śnieżka ombrotrophic peat, where a polluted signal appears in the upper parts of the profile (Fiałkiewicz-Kozieł et al., 2020). These findings set the stage for a more detailed exploration of Pb origin pathways in the following subsections.

Although most of the topsoils are characterized by relatively homogenous Pb isotope signatures, several topsoil samples deviate from this pattern, showing more radiogenic $^{206}Pb/^{207}Pb$ ratios. Some of these values are associated with a stronger

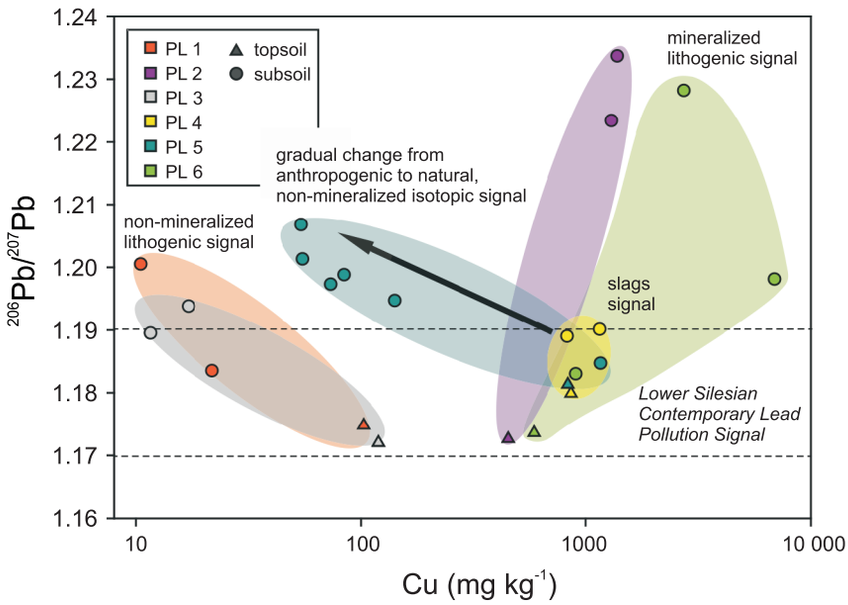

Fig. 6. Trends in $^{206}Pb/^{207}Pb$ ratios as a function of Cu concentration suggesting various Pb pollution origins

Topsoils are characterized by similar isotopic ratios in the range 1.17 and 1.19 (discussed in the next section). Low amounts of Cu in subsoils originating from profiles PL1 and PL3 point to a non-mineralized lithogenic Pb isotopic signal. Copper-rich subsoils (PL2 and PL6) point to a higher Pb isotopic ratio, described as mineralized lithogenic signal. The other profiles are strongly impacted by an isotopic signal originating from slags (PL4, PL5) but present a natural, non-mineralized lithogenic signal in the subsoil (PL5)

lithogenic influence, which is supported by both spatial context and compositional data. SOK8, located on a hill near Cu-rich rock exposures, and SOK4, positioned below slopes containing Cu-mineralized rocks (Fig. 1), likely retain a lithological signal enhanced by weathering of Cu-rich horizons. The elevated $^{206}Pb/^{207}Pb$ in SOK21 closely matches values measured in mineralized rocks, suggesting input from Zechstein Limestone (Ca1) ore in the Kondratów region, where Cu mining and processing also took place. Radiogenic values in other remote samples such as SOK18, and SOK19, where no mineralized rocks exposures occur, may instead reflect inherited sedimentary signals, pre-industrial atmospheric inputs, or subtle variations in local lithology beyond visible ore deposits.

Overall, the isotopic dataset supports a three-endmember mixing model dominated by contributions from local bedrock, metallurgical residues, and an external atmospheric source, with the latter playing a dominant role in surface horizons. A small number of samples hint at additional or more complex Pb inputs which warrant further investigation.

ORE IMPACT ON SUBSOIL ISOTOPIC COMPOSITION

Given the subsurface presence of ore, its influence is expected to be reflected in subsoil Pb isotopic composition (e.g., Walraven et al., 2014). Indeed, rocks, slags and subsoils all exhibit variable $^{206}Pb/^{207}Pb$ ratios, reflecting the complex geological and anthropogenic background of the study area. Oxidized Cu ores, ore-hosting rocks, and historical metallurgical residues all contribute to the local Pb isotopic signature, producing a heterogeneous pattern in the subsoils.

A key trend emerges when examining subsoil data in relation to Cu concentrations (Fig. 6). Soil profiles PL1 and PL3 show relatively low Cu levels and $^{206}Pb/^{207}Pb$ ratios between 1.19 and 1.20. These values are consistent with the regional geogenic background, likely reflecting Pb derived from Quaternary deposits and non-mineralized bedrock in the area (Tyszka et al., 2012, 2016). These profiles are referred to as the 'natural group', characterized by limited influence from copper ores or waste. In contrast, profiles PL2 and PL6 show both elevated Cu concentrations and higher $^{206}Pb/^{207}Pb$ ratios (Fig. 6). These profiles are associated with ore-bearing lithologies, such as Cu-rich slates and marls from the Zechstein Ca1. We classify these as the 'mineralized group', where the isotopic data suggest an admixture of Pb from oxidized Cu ores, which are known to possess radiogenic isotope compositions due to their formation history and U/Pb-rich host rocks (Oszczepalski, 1999; Asael et al., 2012). Two additional profiles, PL4 and PL5, illustrate a third scenario. Both are influenced by historical slags but present different isotopic patterns. PL4 shows a narrow range of $^{206}Pb/^{207}Pb$ values despite high Cu content, pointing to a homogenized slag-derived signal with relatively stable isotopic composition. PL5, in turn, displays stratification: surface layers contain Cu-rich slag-derived contamination with low $^{206}Pb/^{207}Pb$ ratios, while deeper layers show a gradual return towards geogenic values (Fig. 6). This 'hybrid profile' reflects the superposition of metallurgical and geological Pb sources.

Altogether, the subsoils analysed are diverse in Pb isotopic composition and that may be related to the impact of oxidized ores as Pb source in some of the profiles. The fact that the signal is specific for the area studied is corroborated by literature data that did not show similar increase in both Pb isotopic ratios and Cu in subsoils (Kierczak et al., 2013; Tyszka et al., 2016). Observed trends underscore the role of both mineralized bedrock and anthropogenic waste in shaping the subsoil Pb isotopic composition. The distinction between 'natural', 'mineralized', and 'slag-impacted' profiles provides a useful conceptual

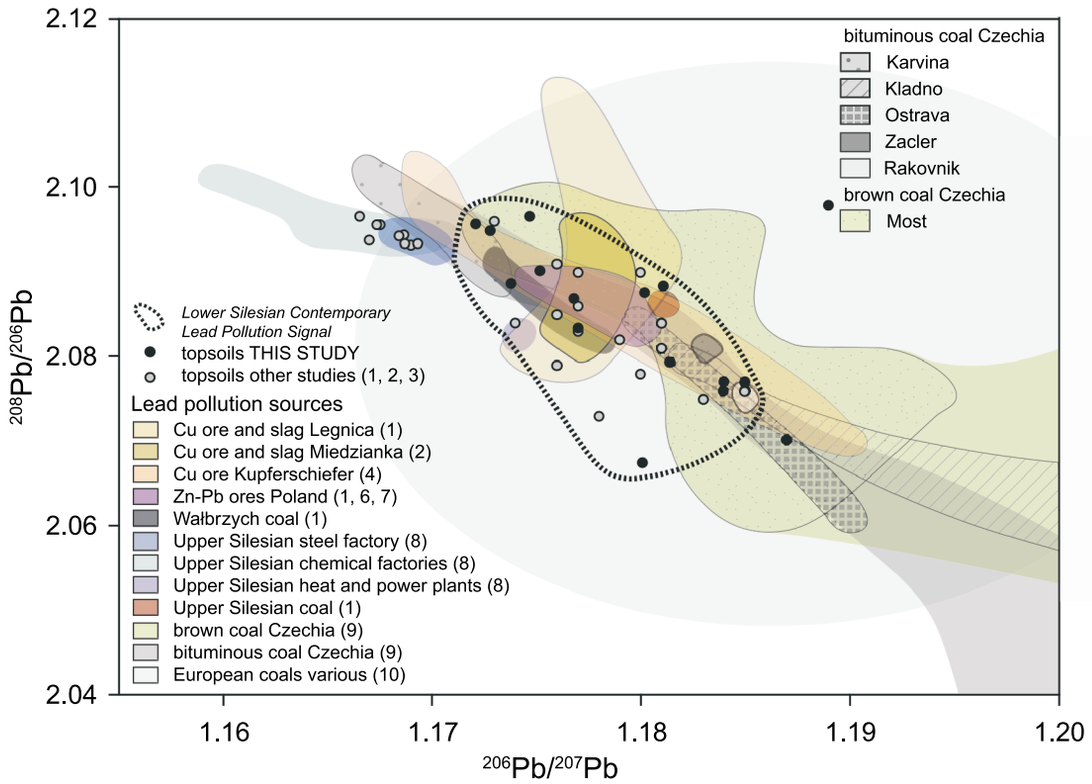

Fig. 7. The Lower Silesian Contemporary Pollution Signal and possible lead sources affecting the $^{206}Pb/^{207}Pb$ and $^{208}Pb/^{206}Pb$ ratios

Topsoils from this study were selected from the set presenting those affected by the LSCPS. Data after (1) Tyszka et al. (2012); (2) Kierczak et al. (2013); (3) Bińczycki et al. (2020); (4) Wedepohl et al. (1978); (5) Church and Vaughn (1992); (6) De Vleeschouwer et al. (2009); (7) Prechova et al. (2023); (8) Sensuła et al. (2021); (9) Mihaljevič et al. (2009); (10) Bi et al. (2017)

framework for understanding Pb mobility and accumulation pathways in mining-impacted terrains. Importantly, the elevated and variable isotopic ratios in subsoils contrast with the homogeneity seen in topsoils, reinforcing the idea that subsoils retain a record of site-specific contamination and geological background, while topsoils are overprinted by widespread atmospheric deposition. This vertical decoupling highlights the value of Pb isotopic profiling in reconstructing past contamination events and identifying localized pollution legacies.

MOBILITY OF LEAD AND ISOTOPIC PATTERNS REVEALED BY EDTA EXTRACTION

The isotopic composition of EDTA-extractable Pb supports a dual-source model: mobile Pb in topsoils mainly derives from atmospheric deposition, whereas immobile Pb in deeper horizons preserves lithogenic and metallurgical signatures. In topsoils, EDTA-leachable $^{206}Pb/^{207}Pb$ ratios form a narrow cluster between 1.17 and 1.19 and are consistently lower than bulk soil values. This suggests that the mobile Pb fraction in surface horizons is isotopically homogenized and largely controlled by anthropogenic atmospheric deposition, which overprints the natural geogenic variability observed in subsoils, in line with Fernández et al. (2008), who observed that EDTA extracts from surface horizons of forest soils contained less radiogenic Pb, consistent with anthropogenic sources.

In contrast, subsoils display a broader isotopic spread, with EDTA-leachable ratios extending from 1.174 up to 1.228. Here, the isotopic signature of the mobile fraction is more profile-specific, reflecting local inputs from bedrock, mineralized lithologies, or metallurgical residues, which echoes the findings of Tyszka et al. (2016), where deeper horizons preserved more variable, lithogenic signals compared to isotopically uniform topsoils. The magnitude and direction of EDTA-bulk offsets also vary among profiles. Natural soils such as PL1 and PL3 show only minor differences, indicating the limited influence of external mobile Pb sources. Mineralized profiles (PL2, PL6) show more pronounced offsets, with EDTA fractions reflecting interaction with radiogenic Pb derived from Cu-enriched lithologies. Slag-impacted profiles (PL4, PL5) reveal a mixed picture: in PL4, EDTA values track the homogenized slag signal, whereas in PL5, EDTA fractions capture the vertical transition from anthropogenic inputs in surface layers toward a geogenic background at depth.

LEAD SOURCES IN TOPSOILS

Consistent lead isotopic signatures in topsoils collectively with Pb concentrations and EDTA-leaching results suggest that the dominant Pb source in topsoil is atmospheric fallout, rather than direct contamination from mining or smelting activities at the site. The vertical gradient in Pb concentration and mobility (based on the EDTA extraction) further supports this interpretation, as deeper soil layers remain relatively unaffected. These isotopic values (1.172–1.180) align closely with Pb isotope ratios reported for topsoils around Lower Silesia and adjacent areas in Czechia (Mihaljevič et al., 2009; Tyszka et al., 2012; Kierczak et al., 2013; Bińczycki et al., 2020). Moreover, such Pb

isotopic composition has been observed in atmospheric fallout in those regions (Komárek et al., 2008; Mihaljevič et al., 2009; Prechova et al., 2023). Similar values were also identified in ombrotrophic peat profiles from the Śnieżka region, where Pb was primarily derived from coal combustion, with gasoline-derived Pb isotopically masked by the dominant coal signal (Fiałkiewicz-Kozieł et al., 2020). The prevalence of the 1.17–1.18 $^{206}Pb/^{207}Pb$ ratio in topsoil across such a wide region is indicative of Pb contributions from a well-mixed atmospheric source. We subsequently refer to this signal as the Lower Silesian Contemporary Pollution Signal (LSCPS), where Pb originates from widespread atmospheric pollution. The LSCPS represents the cumulative atmospheric fallout from several anthropogenic sources active over the past decades. This isotopic fingerprint is consistently found in surface soils (Tyszka et al., 2012; Bińczycki et al., 2020), urban dust (Gmochowska et al., 2019), atmospheric particulates/fly ashes (Tyszka et al., 2016), and even in vegetation (Sensuła et al., 2021) across the region, suggesting a well-mixed and long-range transport mechanism for Pb-bearing particles. The isotopic signature is detected even in relatively enclosed valley settings, underscoring the mobility of atmospheric Pb and its ability to affect remote areas. This supports previous observations in mountainous regions of SW Poland (Bińczycki et al., 2020), where similar Pb ratios were found despite limited local industrial activity.

To put our results in context, we compared the Pb isotope data from topsoil with published values for regional emission sources and mineral deposits (Fig. 7). Notably, published lead isotope data for polluted samples are limited, but a few clear patterns can still be observed. First, Upper Silesian steel factories and chemical plants present distinctly different $^{206}Pb/^{207}Pb$ and $^{208}Pb/^{206}Pb$ ratios from the LSCPS (Sensuła et al., 2021). Secondly, different metallic ores, including Cu ores from the Kupferschiefer deposits, from Miedzianka (older mineralization associated with the Karkonosze-Izera granite intrusion) (Kierczak et al., 2013), Zn-Pb ores from the Silesian-Kraków region (De Vleeschouwer et al., 2009; Prechova et al., 2023) as well as Cu ores and slags associated with the Kupferschiefer (Wedepohl et al., 1978; Tyszka et al., 2012) present fairly similar Pb isotopic compositions. While some overlap exists between the LSCPS and the isotopic signatures of Cu ores and historical slags, the spatial pattern of topsoil contamination and its isotopic homogeneity argue against a local ore-related origin.

Multiple potential contributors to the LSCPS have been determined (Fig. 7). Given the distances between different sources and their suspected presence in the region studied, we identify: 1) bituminous coal combustion in power plants and residential heating (both Polish and Czech sources), 2) metallurgical emissions from smelters in Upper Silesia and the Ostrava-Karviná region, 3) past use of leaded gasoline, particularly during the 20th century. From these potential sources, coal combustion appears to dominate LSCPS, as inferred from both isotopic composition (Fig. 7) and historical emission records (Mihaljevič et al., 2009; Prechova et al., 2023). The $^{206}Pb/^{207}Pb$ range of 1.17–1.19 is characteristic of Polish (from Wałbrzych in Lower Silesia and Upper Silesian) and Czech coal (from Karviná and Ostrava), which possess relatively radiogenic lead isotopic signatures due to the geologic age of the source material. This conclusion is in agreement with previous findings reported by Fiałkiewicz-Kozieł et al. (2020). Also, a recent study from a highly industrial area of Upper Silesia in Poland seems to corroborate this conclusion, as well as suggesting that the LSCPS might be detectable across an even larger area of Poland (Prechova et al., 2023), with a few studies having reported similar Pb isotopic values in topsoils across the country (Tyszka et al., 2012; Reimann et al., 2012; Gałuszka et al., 2018).

ENVIRONMENTAL AND MONITORING IMPLICATIONS

The distribution and isotopic composition of Pb in the study area reflect a complex interplay between source types, vertical soil stratigraphy, and environmental conditions. While isotopic ratios in the topsoils point to a homogeneous, regional pollution signal, and subsoils show lithogenic and slag-related variability, the physical environment likely modulates how these signals are expressed and preserved. Several soil parameters influence the mobility and retention of Pb. Higher cation exchange capacity (CEC), pH variation, moisture conditions and elevated organic matter content in topsoils contribute to Pb accumulation near the surface (Karczewska, 1996; Coles and Yong, 2005; Schwab et al., 2005; Souter and Watmough, 2017; Derkowska et al., 2023). This is supported in our study by the strong positive correlation observed between Pb and total carbon, sulphur, and CEC, suggesting the role of organo-metallic complexes and sorption onto reactive soil components (Derkowska et al., 2023, SM3).

In addition, meteorological and topographic context may play a key role in Pb isotope distribution (Ettler et al., 2011). Leszczyna village is located at the southeastern margin of the NCB, within a valley system surrounded by elevated terrain (Kowalski et al., 2017). While such topography might be expected to shield the area from regional pollution inflows, the consistent presence of the LSCPS even in enclosed sites suggests that long-range atmospheric transport is highly effective. Prevailing winds in the region come predominantly from the south and southwest, facilitating the movement of airborne pollutants from industrial areas of Upper Silesia, Wałbrzych, and Ostrava-Karviná – all known emitters of radiogenic Pb linked to coal combustion (Mihaljevič et al., 2009; Prechova et al., 2023).

Moreover, deposition of atmospheric Pb may be seasonally enhanced during the heating season, when emissions from domestic and industrial coal burning peak. The widespread detection of LSCPS even in low-lying or vegetated areas of the site indicates that particulate-bound Pb can settle under a variety of conditions, overcoming potential barriers imposed by topography. Although this study did not directly integrate wind field data or dispersion models, the isotopic homogeneity observed in the topsoils supports the conclusion that regional-scale atmospheric processes dominate Pb inputs in the surface soil. Future work incorporating high-resolution meteorological modeling and isotope-climate integration could further refine our understanding of depositional dynamics in complex terrain.

Importantly, delineating a regional Pb isotopic signature such as the LSCPS has broader environmental and societal relevance. It can serve as a diagnostic tool in soil monitoring, allowing rapid identification of modern pollution versus legacy contamination. This is particularly valuable in land-use planning and public health assessments: areas dominated by the LSCPS may be prioritized for preventive measures, such as vegetation barriers, soil amendments, or exposure risk communication. Moreover, mapping the spatial extent of this signal across Poland and neighbouring regions could help to identify zones with elevated background pollution, which may otherwise go unnoticed due to the absence of obvious industrial sources. This knowledge can be instrumental in targeting remediation efforts and allocating resources efficiently, especially in vulnerable ecosystems or densely populated areas. From a scientific perspective, understanding the LSCPS also aids in decoupling natural *versus* anthropogenic Pb pools, which is critical for accurate geochemical baselining, climate archives interpretation, or evaluating the long-term fate of atmospheric pollutants in soil systems. The LSCPS thus functions not only as a marker of pollution history but also as a framework for anticipating future environmental and regulatory challenges.

CONCLUSIONS

This study presents an integrated geochemical and isotopic investigation of lead in soils from the historical Old Copper Basin in southwestern Poland. By combining Pb isotope data with elemental concentrations and EDTA-extraction results, we demonstrate a distinct vertical and spatial separation between natural, historical and modern pollution sources.

Topsoils within the study area are characterized by a narrow range of $^{206}Pb/^{207}Pb$ ratios (1.172–1.185), consistent with a widespread regional isotopic signal linked to atmospheric deposition. This isotopic fingerprint, referred to here as the Lower Silesian Contemporary Pollution Signal (LSCPS), reflects cumulative emissions from coal combustion and industrial activities in Poland and Czechia. Its ubiquity, even in semi-enclosed valley settings, underscores the high mobility of airborne Pb and the need to consider regional-scale processes when assessing surface contamination. In contrast, subsoils display greater isotopic diversity and higher $^{206}Pb/^{207}Pb$ values, commonly correlated with elevated Cu concentrations. These results suggest the presence of lithogenic and ore-derived Pb, especially in profiles developed on or near mineralized Zechstein Limestone (Ca1) rocks or contaminated by historical slags. This vertical isotopic decoupling supports the use of Pb isotopes as effective tracers of contamination sources and legacy inputs. The EDTA extraction highlights that Pb mobility is not uniform across the study area. In topsoils it reveals the dominance of isotopically less radiogenic, anthropogenic Pb, whereas in subsoils it exposes the complexity of local lithogenic and waste-derived inputs. This dual control underscores the importance of considering both soil depth and site-specific history when evaluating the mobility and isotopic composition of Pb in contaminated terrains.

Overall, this study demonstrates that even in geologically complex and historically polluted regions, the current Pb isotopic composition in topsoils is largely governed by contemporary atmospheric input. Recognizing and delineating regional isotopic signals like the LSCPS can support environmental monitoring, land-use planning, and targeted remediation, especially in areas where local and regional contamination sources intersect.

Acknowledgements. We would like to acknowledge that funding for the study was provided by the National Science Centre in Poland within Preludium 18 grant to KD, no. 2019/35/N/ST10/04524. The final writing and editing was supported by Polish Geological Institute – National Research Institute statutory funds (Project No. 62.9012.2338.00.0.). The use of LiDAR data in the present study was enabled by the academic license no. DIO.DFT.DSI.7211.1619.2015_PL_N issued to the University of Wrocław, Faculty of Earth Sciences and Environmental Management by the Polish National Head Office of Geodesy and Cartography. We would also like to thank Dr. Marta Prell and Marie Fayadová who helped with sample preparation for the isotopic study, as well as Alice Jarošíková for significant help during the corresponding author's stay in Prague. And finally, we would like to thank our Reviewers who helped to improve the manuscript and its clarity.

REFERENCES

Abbaszade, G., Tserendorj, D., Salazar-Yanez, N., Zacháry, D., Völgyesi, P., Tóth, E., Szabó, C., 2022. Lead and stable lead isotopes as tracers of soil pollution and human health risk assessment in former industrial cities of Hungary. Applied Geochemistry, **145**, 105397; https://doi.org/10.1016/j.apgeochem.2022.105397

Alderton, D.H.M., Selby, D., Kucha, H., Blundell, D.J., 2016. A multistage origin for Kupferschiefer mineralization. Ore Geology Reviews, **79**: 535–543; https://doi.org/10.1016/j.oregeov.2016.05.007

Alyazichi, Y.M., Jones, B.G., McLean, E., 2016. Lead isotope fingerprinting used as a tracer of lead pollution in marine sediments from Botany Bay and Port Hacking estuaries, southern Sydney, Australia. Regional Studies in Marine Science, **7**: 136–141; https://doi.org/10.1016/j.rsma.2016.06.006

Asael, D., Matthews, A., Bar-Matthews, M., Harlavan, Y., Segal, I., 2012. Tracking redox controls and sources of sedimentary mineralization using copper and lead isotopes. Chemical Geology, **310–311**: 23–35; https://doi.org/10.1016/j.chemgeo.2012.03.021

Bi, X., Li, Z., Wang, S., Zhang, L., Xu, R., Liu, R., Yang, H., Guo, M., 2017. Lead isotopic compositions of selected coals, Pb/Zn ores and fuels in China and the application for source tracing. Environmental Science and Technology, **51**: 13502–13508. https://doi.org/10.1021/acs.est.7b04119

Bińczycki, T., Weber, J., Mielnik, L., Asensio, C., 2020. Lead isotope ratios in Podzol profiles as a tracer of pollution source in the subalpine zone of the Karkonosze National Park, Sudety Mts (south-western Poland). Catena, **189**, 104476; https://doi.org/10.1016/j.catena.2020.104476

Cheyne, C.A.L., Thibodeau, A.M., Slater, G.F., Bergquist, B.A., 2018. Lead isotopes as particulate contaminant tracers and chronostratigraphic markers in lake sediments in northeastern North America. Chemical Geology, **477**: 47–57; https://doi.org/10.1016/j.chemgeo.2017.11.043

Church, S.E., Vaughn, R.B., 1992. Lead-isotopic characteristics of the Cracow-Silesia Zn-Pb ores, southern Poland. U.S. Geological Survey, Department of the Interior.

Coles, C.A., Yong, R.N., 2002. Aspects of kaolinite characterization and retention of Pb and Cd. Applied Clay Science, **22**: 39–45; https://doi.org/10.1016/S0169-1317(02)00110-2

De Vleeschouwer, F., Fagel, N., Cheburkin, A., Pazdur, A., Sikorski, J., Mattielli, N., Renson, V., Fialkiewicz, B., Piotrowska, N., Le Roux, G., 2009. Anthropogenic impacts in North Poland over the last 1300 years – a record of Pb, Zn, Cu, Ni and S in an ombrotrophic peat bog. Science of The Total Environment, **407**: 5674–5684; https://doi.org/10.1016/j.scitotenv.2009.07.020

Derkowska, K., Kierczak, J., Potysz, A., Pietranik, A., Pędziwiatr, A., Ettler, V., Mihaljevič, M., 2023. Combined approach for assessing metal(loid)s leaching, mobility and accumulation in a specific near-neutral (pH) environment of a former Cu-smelting area in the Old Copper Basin, Poland. Applied Geochemistry, **148**, 105670; https://doi.org/10.1016/j.apgeochem.2023.105670

Ettler, V., Mihaljevič, M., Komárek, M., 2004. ICP-MS measurements of lead isotopic ratios in soils heavily contaminated by lead smelting: tracing the sources of pollution. Analytical and Bioanalytical Chemistry, **378**: 311–317; https://doi.org/10.1007/s00216-003-2229-y

Ettler, V., Mihaljevič, M., Kříbek, B., Majer, V., Šebek, O., 2011. Tracing the spatial distribution and mobility of metal/metalloid contaminants in Oxisols in the vicinity of the Nkana copper smelter, Copperbelt province, Zambia. Geoderma, **164**: 73–84; https://doi.org/10.1016/j.geoderma.2011.05.014

Fernandez, C., Monna, F., Labanowski, J., Louber, M., van Oort, F., 2008. Anthropogenic lead distribution in soils under arable land and permanent grassland estimated by Pb isotopic compositions. Environmental Pollution, **156**: 1083–1091; https://doi.org/10.1016/j.envpol.2008.04.014

Fiałkiewicz-Kozieł, B., Łokas, E., Gałka, M., Kołaczek, P., De Vleeschouwer, F., Le Roux, G., Smieja-Król, B., 2020. Influence of transboundary transport of trace elements on mountain peat geochemistry (Sudetes, Central Europe), Quaternary Science Reviews, **230**, 106162; https://doi.org/10.1016/j.quascirev.2020.106162

Gałuszka, A., Migaszewski, Z.M., Dołęgowska, S., Michalik, A., 2018. Geochemical anomalies of trace elements in unremediated soils of Mt. Karczówka, a historic lead mining area in the city of Kielce, Poland. Science of The Total Environment, **639**: 397–405; https://doi.org/10.1016/j.scitotenv.2018.05.174

Głuszyński, A., Aleksandrowski, P., 2022. Late Cretaceous–early Palaeogene inversion-related tectonic structures at the north-eastern margin of the Bohemian Massif (southwestern Poland and northern Czechia). Solid Earth, **13**: 1219–1242; https://doi.org/10.5194/se-13-1219-2022

Gmochowska, W., Pietranik, A., Tyszka, R., Ettler, V., Mihaljevič, M., Długosz, M., Walenczak, K., 2019. Sources of pollution and distribution of Pb, Cd and Hg in Wrocław soils: Insight from chemical and Pb isotope composition. Geochemistry, **79**: 434–445; https://doi.org/10.1016/j.chemer.2019.07.002

Kabata-Pendias, A., Szteke, B., 2015. Trace Elements in Abiotic and Biotic Environments. CRC Press, Taylor and Francis Group, Boca Raton.

Kądziołka, K., Kierczak, J., Pietranik, A., 2019. Mineralogical characteristics of metallic phases in copper slags from the Old Copper Basin, Poland (in Polish with English summary). Przegląd Geologiczny, **67**: 164–166; https://doi.org/10.7306/2019.9

Kądziołka, K., Pietranik, A., Kierczak, J., Potysz, A., Stolarczyk, T., 2020. Towards better reconstruction of smelting temperatures: Methodological review and the case of historical K-rich Cu-slags from the Old Copper Basin, Poland. Journal of Archaeological Science, **118**, 105142; https://doi.org/10.1016/j.jas.2020.105142

Kierczak, J., Potysz, A., Pietranik, A., Tyszka, R., Modelska, M., Neel, C., Ettler, V., Mihaljevič, M., 2013. Environmental impact of the historical Cu smelting in the Rudawy Janowickie Mountains (South-Western Poland). Journal of Geochemical Exploration, **124**: 183–194; https://doi.org/10.1016/j.gexplo.2012.09.008

Komárek, M., Ettler, V., Chrastný, V., Mihaljevič, M., 2008. Lead isotopes in environmental sciences: a review. Environment International, **34**: 562–577; https://doi.org/10.1016/j.envint.2007.10.005

Kowalski, A., Maciejak, K., Wojewoda, J., Kozłowski, A., Raczyński, P., 2017. Anthropogenic changes of the "Old Copper Basin" area landscape (North-Sudetic Synclinorium) in the light of LiDAR-based geomorphometric analysis and archival data (in Polish with English summary). Biuletyn Państwowego Instytutu Geologicznego, **469**: 177–200; https://doi.org/10.5604/01.3001.0010.0080

Kryza, R., Mazur, S., Oberc-Dziedzic, T., 2004. The Sudetic geological mosaic: Insights into the root of the Variscan orogeny. Przegląd Geologiczny, **52**: 761–773.

Leszczyński, S., Nemec, W., 2019. Sedimentation in a synclinal shallow-marine embayment: Coniacian of the North Sudetic Synclinorium, SW Poland. The Depositional Record, **6**: 144–171; https://doi.org/10.1002/dep2.92

Mihaljevič, M., Ettler, V., Strnad, L., Šebek, O., Vonásek, F., Drahota, P., Rohovec, J., 2009. Isotopic composition of lead in Czech coals. International Journal of Coal Geology, **78**: 38–46; https://doi.org/10.1016/j.coal.2008.09.018

Mihaljevič, M., Ettler, V., Šebek, O., Sracek, O., Kříbek, B., Kyncl, T., Majer, V., Veselovský, F., 2011. Lead isotopic and metallic pollution record in tree rings from the Copperbelt mining–smelting area, Zambia. Water, Air and Soil Pollution, **216**: 657–668; https://doi.org/10.1007/s11270-010-0560-4

Milewicz, J., 1985. Development of the Rotliegendes in south-western Poland (in Polish with English summary). Geological Quarterly, **29** (4): 679–690.

Monna, F., Aiuppa, A., Varrica, D., Dongarra, G., 1999. Pb isotope composition in lichens and aerosols from eastern Sicily: Insights into the regional impact of volcanoes on the environment. Environmental Science & Technology, **33**: 2517–2523; https://doi.org/10.1021/es9812251

Oszczepalski, S., 1999. Origin of the Kupferschiefer polymetallic mineralization in Poland. Mineralium Deposita, **34**: 599–613; https://doi.org/10.1007/s001260050222

Peng, B., Chen, H., Fang, X., Xie, S., Wu, S., Jiang, C., Dai, Y., 2022a. Distribution of Pb isotopes in different chemical fractions in bed sediments from lower reaches of the Xiangjiang River, Hunan Province of China. Science of The Total Environment, **829**, 154394; https://doi.org/10.1016/j.scitotenv.2022.154394

Peng, B., Juhasz, A., Fang, X., Jiang, C., Wu, S., Li, X., Xie, S., Dai, Y., 2022b. Lead isotopic fingerprinting as a tracer to identify the sources of heavy metals in sediments from the Four Rivers' inlets to Dongting Lake, China. Catena, **219**, 106594; https://doi.org/10.1016/j.catena.2022.106594

Potysz, A., Kierczak, J., Pietranik, A., Kądziołka, K., 2018. Mineralogical, geochemical, and leaching study of historical Cu-slags issued from processing of the Zechstein formation (Old Copper Basin, southwestern Poland). Applied Geochemistry, **98**: 22–35; https://doi.org/10.1016/j.apgeochem.2018.08.027

Prechova, E., Sebek, O., Novak, M., Andronikov, A.V., Strnad, L., Chrastny, V., Cabala, J., Stepanova, M., Pasava, J., Martinkova, E., Pacherova, P., Blaha, V., Curik, J., Veselovsky, F., Vitkova, H., 2023. Spatial and temporal trends in ^{66}Zn and $^{206}Pb/^{207}Pb$ isotope ratios along a rural transect downwind from the Upper Silesian industrial area: Role of legacy vs. present-day pollution. Environmental Pollution, **328**, 121609; https://doi.org/10.1016/j.envpol.2023.121609

Quevauviller, P., 1998. Operationally defined extraction procedures for soil and sediment analysis I. Standardization. TrAC Trends in Analytical Chemistry, **17**: 289–298.

Raczyński, P., 2010. North-Sudetic Basin: nearshore carbonate and siliciclastic deposits. In: Petroleum Geological Atlas of the Southern Permian Basin Area (eds. J.C. Doornenbal and A.G. Stevenson): 142–143. EAGE Publications b.v, Houten.

Reimann, C., Flem, B., Fabian, K., Birke, M., Ladenberger, A., Négrel, P., Demetriades, A., Hoogewerff, J., 2012. Lead and lead isotopes in agricultural soils of Europe – The continental perspective. Applied Geochemistry, **27**: 532–542; https://doi.org/10.1016/j.apgeochem.2011.12.012

Schwab, A.P., He, Y., Banks, M.K., 2005. The influence of organic ligands on the retention of lead in soil. Chemosphere, **61**: 856–866; https://doi.org/10.1016/j.chemosphere.2005.04.098

Sensuła, B., Fagel, N., Michczyński, A., 2021. Radiocarbon, trace elements and Pb isotope composition of pine needles from a highly industrialized region in southern Poland. Radiocarbon, **63**: 713–726; https://doi.org/10.1017/RDC.2020.132

Sipos, P., Németh, T., Kovács Kis, V., 2013. Lead isotope composition and host phases in airborne particulate matter from Budapest, Hungary. Central European Geology, **56**: 39–57; https://doi.org/10.1556/ceugeol.56.2013.1.4

Souter, L., Watmough, S.A., 2017. Geochemistry and toxicity of a large slag pile and its drainage complex in Sudbury, Ontario. Science of The Total Environment, **605–606**: 461–470; https://doi.org/10.1016/j.scitotenv.2017.06.237

Tyszka, R., Pietranik, A., Kierczak, J., Ettler, V., Mihaljevič, M., Weber, J., 2012. Anthropogenic and lithogenic sources of lead in Lower Silesia (Southwest Poland): an isotopic study of soils, basement rocks and anthropogenic materials. Applied Geochemistry, **27**: 1089–1100; https://doi.org/10.1016/j.apgeochem.2012.02.034

Tyszka, R., Pietranik, A., Kierczak, J., Ettler, V., Mihaljevič, M., 2014. Extensive weathering of zinc smelting slag in a heap in Upper Silesia (Poland): Potential environmental risks posed by mechanical disturbance of slag deposits. Applied Geochemistry, **40**: 70–81; https://doi.org/10.1016/j.apgeochem.2013.10.010

Tyszka, R., Pietranik, A., Kierczak, J., Ettler, V., Mihaljevič, M., Medyńska-Juraszek, A., 2016. Lead isotopes and heavy minerals analyzed as tools to understand the distribution of lead and other potentially toxic elements in soils contaminated by Cu smelting (Legnica, Poland). Environmental Science and Pollution Research, **23**: 24350–24363; https://doi.org/10.1007/s11356-016-7655-4

Walraven, N., van Os, B.J.H., Klaver, G.Th., Middelburg, J.J., Davies, G.R., 2014. The lead (Pb) isotope signature, behaviour and fate of traffic-related lead pollution in roadside soils in The Netherlands. Science of The Total Environment, **472**: 888–900; https://doi.org/10.1016/j.scitotenv.2013.11.110

Wedepohl, K.H., Delevaux, M.H., Doe, B.R., 1978. The potential source of lead in the Permian Kupferschiefer bed of Europe and some selected Paleozoic mineral deposits in the Federal Republic of Germany. Contributions to Mineralogy and Petrology, **65**: 273–281; https://doi.org/10.1007/BF00375513

Yang, Y., Li, S., Bi, X., Wu, P., Liu, T., Liu, C., 2010. Lead, Zn, and Cd in slags, stream sediments, and soils in an abandoned Zn smelting region, southwest China, and Pb and S isotopes as source tracers. Journal of Soils and Sediments, **10**: 1527–1539. https://doi.org/10.1007/s11368-010-0234-7